International Journal
of
Integrated Sciences & Technology (IJIST)
http://www.cuet.ac.bd/IJIST/index.html

International Journal of Integrated Sciences & Technology 2 (2016) 7-13

First-principles Studies of the Structural, Elastic, Electronic and Optical Properties of Ti_2CdC and Ti_2CdN

M. Roknuzzaman[2]*, M. A. Hadi[2] and M. J. Abden[2]

[1]*Department of Physics, Jessore University of Science and Technology, Jessore 7408, Bangladesh*
[2]*Department of Physics, Rajshahi University, Rajshahi 6205, Bangladesh*
[3]*Department of EEE, International Islamic University Chittagong, Chittagong 4203, Bangladesh*

Abstract

First-principles studies were conducted to investigate the structural, elastic, electronic and optical properties of the Cd-containing only synthesized MAX phase Ti_2CdC in comparison with the predicted phase Ti_2CdN. Our calculations show that the substitution of C by N in Ti_2CdC mostly affects the lattice constant *c* but the lattice constant *a* almost remains unchanged. All elastic constants and moduli increase when C is replaced by N. In comparison with the Ti_2CdN phase, Ti_2CdC is more compressible along the c-axis. The elastic anisotropy in Ti_2CdC is high in comparison with Ti_2CdN. Both nanolaminates are brittle in nature. The calculated electronic band structures and density of states imply that the chemical bonding in two compounds is a combination of covalent, ionic and metallic nature. Ti_2CdC is more conducting than Ti_2CdN. The obtained reflectivity spectra show that the MAX phases Ti_2CdC and Ti_2CdN have the potential to be used as coating materials for reducing solar heating.

Keywords: First principles, elastic properties, electronic properties, optical properties.

1. Introduction

The MAX phases, a class of layered ternary carbides and nitrides, are described by the chemical formula $M_{n+1}AX_n$, with the different MAX stoichiometries often referred to as 211, 312, and 413 phases for n = 1, 2, and 3, respectively. In the periodic table of elements, M is an early transition metal from groups 3 (Sc), 4 (Ti, Zr, Hf), 5 (V, Nb, Ta), or 6 (Cr, Mo), A is an A-group element from groups 12 (Cd), 13 (Al, Ga, In, Tl), 14 (Si, Ge, Sn, Pb), 15 (P, As), or 16 (S), and X is C and/or N. The MAX phases are thermodynamically stable nanolaminates which have the potential for industrial applications owing to their conspicuous combination of physical, chemical, electrical, and mechanical properties, some of which are characteristics of metals and ceramics [1]. Due to their simultaneous metallic and ceramics characteristics, the MAX phases are also termed as metallic ceramics [2]. These technologically important ceramics have drawn sufficient attention of material scientists, physicists, and chemists because of their good electrical and thermal conductivities, exceptional damage tolerance, good machinability, excellent thermal shock resistance, fully reversible plasticity, high resistance to oxidation and corrosion, good elastic rigidity, and ability to maintain the strengths to high temperature [2-9].

Among the known 85 synthesized MAX compounds [10], only Ti_2CdC phase contains Cd as A-group element. Moreover, this material is synthesized at the early period of discovery of the MAX phases by their discoverers' group [11]. Inspite of that Ti_2CdC is, up to date, a relatively little studied member of 211 phases. Liu et al. [12] carried out a theoretical study on structural and mechanical properties of Ti_2CdC along with other Ti_2AC (A = Sn, Ga, In, and Pb) phases. An ab initio study is accomplished by Bai et al. [13] to evaluate the chemical bonding by means of density of states (DOS) and the elastic properties of Ti_2CdC, providing the structural parameters. Yang et al. [14] investigated the dielectric function as optical property of Ti_2CdC including other MAX phases Ti_2AC (A = In, Sn, Al, and Pb). On the other hand, after a theoretical prediction by calculating the elastic coefficients of Ti_2CdN as a stable nanolaminate [15], this phase has not drawn any attention

Corresponding author:
E-mail : rokonphy@yahoo.com
For color version visit: http://www.cuet.ac.bd/IJIST/index.html

from either the experimentalists or the theorists. These motivate us to perform the present study on the structural, elastic, electronic, and optical properties of these Cd-containing MAX phases. We have also shed light on the effect of substitution of C by N in Ti_2CdC phase.

2. Theoretical Methods

The first-principles investigations have been conducted by using the Cambridge Serial Total Energy Package (CASTEP) code [16] in which the plane-wave pseudopotential total energy calculation approach based on the density functional theory (DFT) [17,18] is applied. The electronic exchange-correlation energy has been treated according to Perdew-Burke-Ernzerhof generalized gradient approximation (PBE-GGA) [19]. Interactions of electrons with ion cores were represented by the Vanderbilt-type ultrasoft pseudopotential [20]. To determine the number of plane-waves in expansion, a plane-wave cutoff energy of 500 eV was employed throughout the calculations. The crystal structures were fully optimized to calculate the ground state various properties by independently modifying the lattice parameters and internal atomic coordinates with no core correction or spin effect. The geometry optimizations were acquired through minimizing the total energy and internal forces by using the Broyden-Fletcher-Goldfarb-Shanno (BFGS) minimization technique [21]. The convergence criteria were chosen as the difference in total energy being less than 5 x 10^{-6} eV/atom, the maximum ionic Hellmann -Feyman force being less than 0.01 eV/Å, maximum ionic displacement being less than 5 x 10^{-4} Å, and the maximum stress being less than 0.02 GPa. The tolerance in the self-consistent field calculation was set to 5 x 10^{-7} eV/atom. For the sampling of the Brillouin zone, the Monkhorst-Pack scheme [22] is used to produce a uniform grid of k-points along the three axes in reciprocal space of crystal, and 15 × 15 × 3 k-points for both Ti_2CdC and Ti_2CdN were taken to achieve the ground-states. In optical properties calculations, the Vanderbilt-type ultrasoft pseudopotential was replaced by the norm-conserving pseudopotential remaining the other set up unchanged.

The elastic constants have been determined by applying a set of finite homogeneous deformations and calculating the resulting stresses with respect to optimizing the internal degrees of freedom [23], as implemented in the CASTEP code.

The intraband contribution to the optical properties of metallic compounds like MAX phases affects mainly the low-energy part of the spectra. It can be corrected for dielectric function via including an empirical Drude term [24, 25] with unscreened plasma frequency 3.0 eV and damping 0.05 eV.

The imaginary part $\varepsilon_2(\omega)$ of the dielectric function has been calculated by the formula:

$$\varepsilon_2(\omega) = \frac{2e^2\pi}{\Omega\varepsilon_0} \sum_{k,v,c} \left| \left\langle \psi_k^c \left| \hat{u} \cdot \vec{r} \right| \psi_k^v \right\rangle \right|^2 \delta(E_k^c - E_k^v - E) \quad (1)$$

where is the primitive cell volume, ω is the frequency of light, e is the electronic charge, u is the vector defining the polarization of the incident electric field and ψ_k^c and ψ_k^v are the conduction and valence band wave functions at k, respectively. The Kramers-Kronig relations provide the real part $\varepsilon_1(\omega)$ of the dielectric function and reflectivity.

3. Results and Discussion

3.1. Structural Properties:

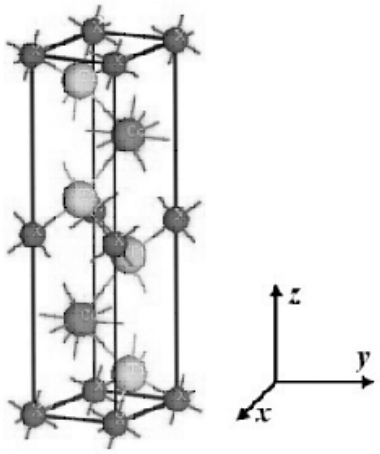

Fig. 1. Crystal structure of Ti_2CdX (X = C, N).

The MAX compounds Ti_2CdC and Ti_2CdN considered in this study belong to the hexagonal crystallographic system with space group $P6_3/mmc$ (No. 194). There are two formula units and eight atoms per unit cell (Fig. 1). Fully relaxed structures for both layered nanolaminates are obtained by optimizing the geometry structure including lattice constants and internal atomic positions, starting from an eight atoms unit cell. The optimized Ti atom located on the 4*f* Wyckoff position, fractional coordinates (1/3, 2/3, 0.077) and (1/3, 2/3, 0.076) in Ti_2CdC and Ti_2CdN, respectively. The Cd atoms are positioned in the 2*d* Wyckoff site, fractional coordinates (1/3, 2/3, 3/4) in Ti_2CdC and Ti_2CdN. The C and N atoms are situated in the 2*a* Wyckoff position, fractional coordinates (0, 0, 0) and (0, 0, 0). The obtained lattice constants a and c, internal atomic coordinate z, equilibrium unit cell volume V, Bulk modulus, and pressure derivative of bulk

modulus *B* for Ti_2CdC and Ti_2CdN at 0K are given in Table 1. Our calculated structural parameters agree quite well with both experimental (where applicable) and theoretical values; the deviations for the lattice constants and volumes are 1.11% and 1.39%, respectively. As noted from the calculated data, the substitution of C by N mostly affects the *c* values; the *a* values almost remain unchanged, which is the opposite of the general trend as C is replaced by N results in a more affected *a* values in comparison with the *c* values [26]. To better understand this intriguing discrepancy more work, especially theoretical work, is required. The bulk modulus increases by 12.5% as the C is substituted with N.

Table 1. Calculated lattice parameters *a* and *c* (in Å), hexagonal ratio *c/a*, internal parameter *z.*, unit cell volume V (in $Å^3$) and bulk modulus B (in GPa) and its pressure derivative B for Ti_2CdC and Ti_2CdN.

Compound	*a*	*c*	*c/a*	*z*	*V*	*B*	*B′*	Reference
Ti_2CdC	3.103	14.57	4.696	0.077	121.50	112	4.9	Present
	3.099	14.41	4.650	0.086	119.84	-	-	Expt. [11]
	3.091	14.528	4.700	-	120.21	-	-	Theo. [12]
	3.104	14.55	4.687	0.077	121.40	116	-	Theo. [13]
	3.106	14.54	4.681	-	121.47	116	-	Theo. [15]
Ti_2CdN	3.078	14.19	4.610	0.076	116.48	126	5.4	Present
	3.082	14.15	4.591	-	116.40	130	-	Theo. [15]

3.2. Elastic Properties

Table 2 lists the calculated elastic constants C_{ij}, together with other theoretical results of Ti_2CdC and Ti_2CdN. Our calculated results for both nanolaminates agree well with the values found in literatures [12,13,15]. The calculated elastic constants are positive and satisfy the well-established Born criteria [27], which suggests that the studied two 211 MAX phases are mechanically stable. It is observed that the elastic constants C_{11} and C_{33} increase when C is substituted with N. So, we may conclude that the Ti-N bonds are stronger than Ti-C bonds. The average difference between C_{11} and C_{33} for all studies of Ti_2CdC is 51.5, whereas for Ti_2CdN, this is 33. It suggests that the elastic anisotropy in Ti_2CdC is high in comparison with Ti_2CdN. Beside this, the calculated shear anisotropy factor, defined by $A = 4C_{44}/(C_{11} + C_{33} - 2C_{13})$, also implies that Ti_2CdC possesses large anisotropy compared to Ti_2CdN for the shear planes {1 0 1 0} between the directions <0 1 1 1> and <0 1 1 0>. The large anisotropy for Ti_2CdC indicates that the in-plane and out - of - plane inter - atomic interactions in Ti_2CdC crystal differ largely. Another anisotropy parameter defined by the ratio between the linear compressibility coefficients along the c- and a-axis for hexagonal crystal: $k_c/k_a = (C_{11} + C_{12} - 2C_{13})/(C_{33} - C_{13})$ has also been evaluated. The obtained results imply that the compressibility along the c-axis is larger than that along the a-axis for both the phases. But in comparison with the Ti_2CdN phase, Ti_2CdC is more compressible along the c-axis. As noted above, the elastic anisotropy decreases as C is replaced by N. In fact, the elastic anisotropy for Ti_2CdN is quite mild and as a result, this phase is almost cubic in its lack of elastic anisotropy [26].

Table 2 also tabulates the values of bulk moduli *B*, shear moduli *G*, Young moduli *Y* and Poisson's ratio *v* of two compounds. For comparison, other theoretical values available in the literatures [12,13,15] are also listed in the table. Not surprisingly, all elastic constants and moduli increase when C is replaced by N. The bulk materials can be classified into two groups according to the Pugh's criteria [28]: ductile and brittle materials. A material should be brittle if its $G/B > 0.5$, otherwise it should

Table 2. Calculated elastic constants Cn_{ij} (GPa), bulk moduli *B* (GPa), shear moduli *G* (GPa), Young's moduli *Y* (GPa), Poisson's ratio *v*, elastic anisotropic factor *A* and k_c/k_a of Ti_2CdC and Ti_2CdN.

Compound	C_{11}	C_{12}	C_{13}	C_{33}	C_{44}	*B*	*G*	*Y*	*G/B*		*A*	k_c/k_a	Ref.
Ti_2CdC	257	68	44	205	36	114	64	162	0.56	0.26	0.385	1.472	Present
	263	64	45	212	39	114	74	183	0.65	0.23	0.405	1.419	Theo.[12]
	258	68	46	205	33	116	70	174	0.60	0.25	0.356	1.465	Theo.[13]
	253	71	47	203	31	116	67	168	0.58	0.26	0.343	1.474	Theo.[15]
Ti_2CdN	266	76	56	235	74	127	87	212	0.68	0.22	0.761	1.285	Present
	270	83	58	235	68	130	84	208	0.65	0.23	0.699	1.339	Theo.[15]

be ductile. The Poisson's ratio for a ductile metallic material is typically 0.33 and for brittle material, it is small and less than 0.33 [29]. So, according to Pugh's criteria and the values of Poisson's ratio, both Ti_2CdC and Ti_2CdN are brittle in nature, which is the general trend of MAX phases [30-32].

3.3. Electronic Properties

The investigated band structures of Ti_2CdC and Ti_2CdN at equilibrium lattice parameters along the high symmetry directions in the first Brillouin zone are illustrated in Fig. 2. The Fermi level of both

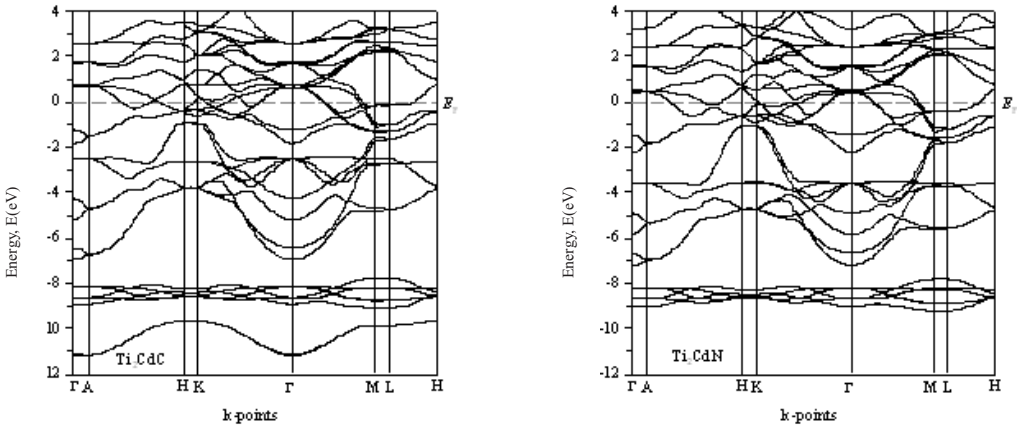

Fig. 2. Electronic band structure of (a) Ti_2CdC and (b) Ti_2CdN with equilibrium optimized structure.

nanolaminates lies above the valence band maximum near the K point. The occupied valence bands of Ti_2CdC lie in the energy range from -6.9 eV to Fermi level E_F. On the other hand, in Ti_2CdN the valence bands extend widely from -7.2 eV to Fermi level. Moreover, for both the phases, a lot of valence bands go across the Fermi level and overlap with conduction bands. Consequently, no band gap is found at the Fermi level and Ti_2CdC as well as Ti_2CdN shows the metallic conductivity.

The total and partial density of states (DOS) of Ti_2CdC and Ti_2CdN are presented in Fig. 3. It is seen that the lowest-lying valence bands in Ti_2CdC, from -11.5 to -9.4 eV, are formed by the C 2*s* states with a small mixture of the Ti 3*p* and Ti 3*d* states. The highest valence bands occupied the energy range from -9.4 to -7.2 eV are derived almost entirely from Cd 4*d* states. The valence bands located between -7.2 and -5.4 eV below the Fermi level arise mainly from mixed Ti 3*s*, 3*p* and Cd 5*s*, 5*p* states. An intense peak in the total DOS in the range -5.4 to -2 eV are originated from the strong hybridization of Ti 3*d* and C 2*p* states indicating the covalent Ti-C bonds in Ti_2CdC. At the Fermi level, the DOS mainly arises from the Ti 3*d* states. The calculated DOSs at the Fermi level $N(E_F)$ is 5.63 states per unit cell per eV, which is high and inherently, explain the metallic behavior of the phase Ti_2CdC. Our result is consistent with the value of 5.595 states per unit cell per eV calculated by Bai et al. [13].The conduction properties of Ti_2CdC results in due to the Ti 3*d* contribution. There is no contribution to the DOS at the Fermi level from C and therefore C is not involved in the conduction properties. A poor contribution from Cd 5*p* states participate in formation of DOS at the Fermi level. These results are consistent with the reports published on MAX phases [31, 33]. The almost similar features are found in Ti_2CdN phase though the lowest-lying valence bands disappear in Ti_2CdC when C is substituted by N. However, the DOSs at the Fermi level decrease from 5.63 to 4.57 states per unit cell per eV as C is replaced with N, indicating that Ti_2CdC is more conducting than Ti_2CdN. This is consistent with the results observed in Ti_2AlX [34,35] and Ti_2InX [36], but not in agreement with the calculations conducted for Ti_2AlX by Du et al. [37] and for Ti_2InX by Benayad et al. [38], where X is C or N. By comparing Figs. 3(a) and 3(b), it is seen that the covalent Ti-C bond in Ti_2CdC has the energy range from -5.4 to -2 eV, whereas the covalent Ti-N bond in Ti_2CdN occupies the energy range from -7.2 to 4 eV. Obviously, the Ti-N bond is stronger than Ti-C bond, since the former appears at a lower energy. For this reason, all elastic moduli of Ti_2CdN are larger than that of Ti_2CdC. The Ti-Cd bonds in both Ti_2CdC and Ti_2CdN correspond to the peaks of states at around -0.34 and -0.76 eV, respectively, which essentially suggest that the Ti-Cd bonds are weaker than Ti-C and Ti-N bonds. The overall bonding character in two MAX phases may be described as a mixture of metallic, covalent and ionic.

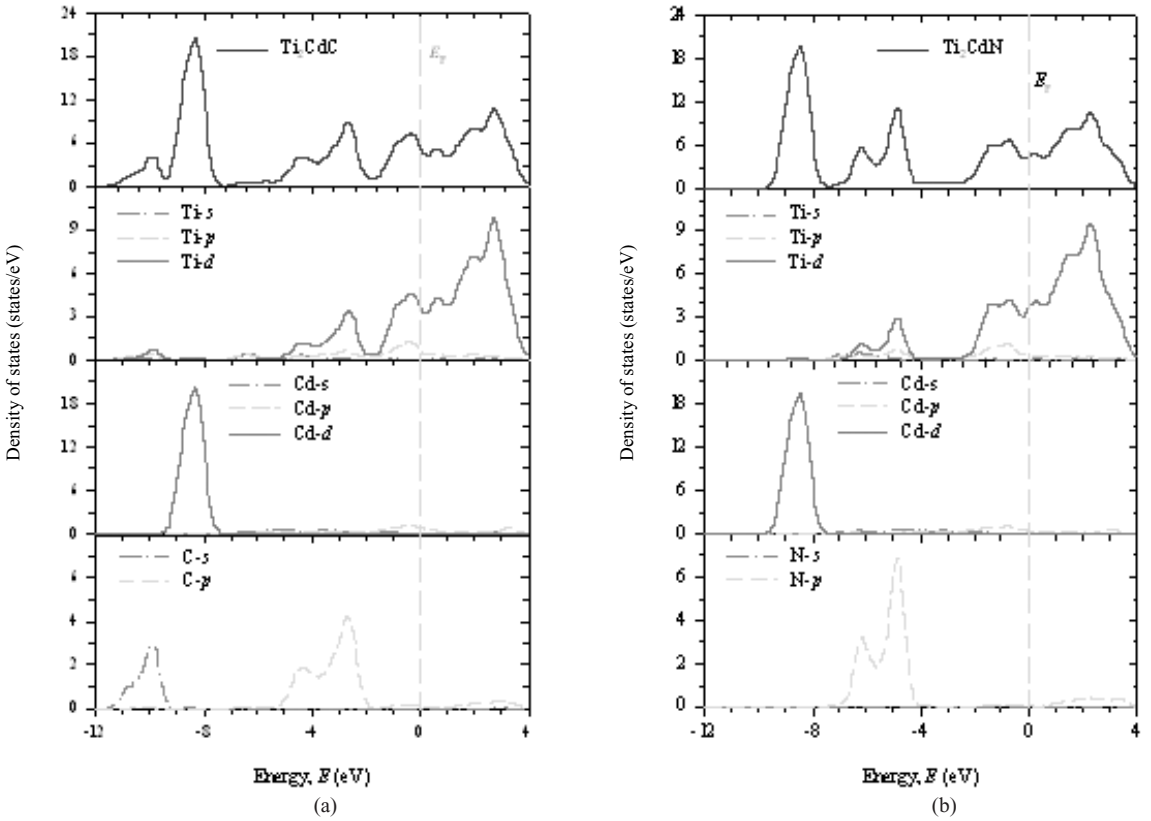

Fig. 3. The calculated total and partial-density of states for (a) Ti_2CdC and (b) Ti_2CdN.

3.5. Optical Properties

The calculated optical properties such as dielectric function and reflectivity of two MAX compounds for incident photon energies up to 20 eV for two polarization vectors [100] and [001] are depicted in Fig. 4. Dielectric function is the most general property of a material, which modifies the incident electromagnetic wave of light. The real and imaginary parts of the dielectric function are illustrated in Figs. 4(a) and 4(b). The real part of the dielectric function ε_1 (ω) of the phase Ti_2CdC for the polarization along [100] direction exhibit two peaks at around 0.8 and 2.3 eV, whereas for [001] direction no peak is found.

In case of Ti_2CdN, a peck is observed at 0.88 eV for the direction [100] and at 1.1 eV for the direction [001]. It is seen that the peak intensity increase expeditiously when C is replaced with N in Ti_2CdC. In the range of $\varepsilon_1 < 0$, the real part of the dielectric function goes through zero from below, which implies

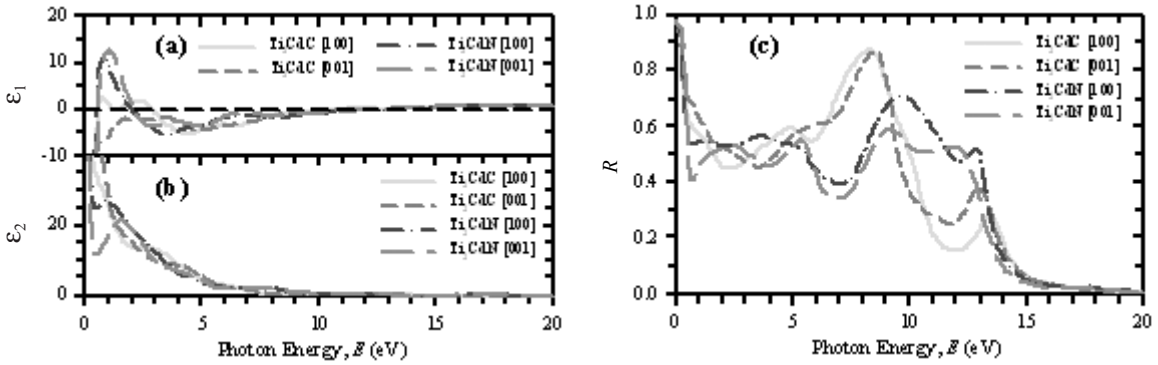

Fig. 4. **(a)** real part of dielectric function, (b) imaginary part of dielectric function and (c) reflectivity of Ti_2CdC and Ti_2CdN.

the metallic nature of the two studied phases. The imaginary part of the dielectric function approaches zero from above that also confirms the metallic characteristics of the two compounds. In fact, this is the general feature of the MAX phase compounds [25, 31, 32, 39]. In the range of high energies, the real part of the dielectric function tends to be unity and the imaginary part reaches nearly zero. It means that in this region where the materials become almost transparent with a small absorption.

The reflectivity spectra as a function of incident photon energy are plotted in Fig. 4(c) for two polarization directions. It is observed that the reflectivity spectra for two different polarization directions do not exhibit great changes in the entire energy range in case of each phase. But the scenario is different for two different phases. At around 4.5 eV a gradual increase starts for Ti_2CdC but a rapid decrease occurs in reflectivity spectra of Ti_2CdN. An intense peak observed at around 8.5 eV in the reflectivity spectra of Ti_2CdC is shifted at around 9.8 eV when C is replaced with N. In the moderate-infrared region, the reflectivity spectra of both MAX materials increase drastically and rise to reach the maximum value of 0.98. It is seen that the reflectivity spectra for two polarization directions for two phases exhibit no significant change in the energy range 1.8-5.1 eV and the amount of reflectivity is always above 44%. Due to almost constant reflectance in the visible light region (1.8-3.1 eV), the two nanolaminates Ti_2CdC and Ti_2CdN should appear as metallic gray. Moreover, for the same reason, the two MAX compounds show the nonselective characteristic that makes them capable of reducing solar heating. So, we may conclude as Li et al. [25] that the MAX phases have the potential to be used as a coating on spacecraft to avoid solar heating.

4. Conclusion

We have performed the first-principles calculations to investigate the structural, elastic, electronic and optical properties of the Cd-containing MAX phase Ti_2CdC and Ti_2CdN. Our results show that the substitution of C by N in Ti_2CdC affects the all properties such as structural, elastic, electronic, etc. The replacement of C with N reduces all the elastic constants and moduli of Ti_2CdC. The phase Ti_2CdC is more compressible along the c-axis compared to Ti_2CdN. The elastic anisotropy of Ti_2CdC is higher than that of Ti_2CdN. The studied two MAX phases are brittle in nature. Via the calculation of electronic band structures and density of states, the chemical bonding in two nanolaminates are seen to be a combination of covalent, ionic and metallic nature. Ti_2CdC is more conducting than Ti_2CdN. The MAX phases Ti_2CdC and Ti_2CdN are potential candidate materials for coating to reduce solar heating.

References

1. M. W. Barsoum, Prog. Solid State Chem. 28, 201 (2000).
2. Z. M. Sun, H. Hashimoto, Z. F. Zhang, S. L. Yang and S. Tada, Mater. Trans. 47, 170 (2006).
3. M. W. Barsoum and T. El-Raghy, J. Am. Ceram. Soc. 79, 1953 (1996).
4. H. Yoo, M.W. Barsoum and T. El-Raghy, Nature (London). 407, 581 (2000).
5. M. W. Barsoum, L. Farber and T. El-Raghy, Metall. Mater. Trans. A 30, 1727 (1999).
6. T. El-Raghy, M.W. Barsoum, A. Zavaliangos and S.R. Kalidindi, J. Am. Ceram. Soc. 82, 2855 (1999).
7. M. Sundberg, G. Malmqvist, A. Magnusson and T. El-Raghy, Ceram. Inter. 30, 1899 (2004).
8. V. D. Jovic, M. W. Barsoum, B. M. Jovic, S. Gupta and T. El-Raghy, Corr. Sci. 48, 4274 (2006).
9. P. Finkel, M. W. Barsoum and T. El-Raghy, J. Appl. Phys. 87, 1701 (2000).
10. A. M. Farle, S. Van der Zwaag and W.G. Sloof, "A conceptual study into the potential of max-phase ceramics for self-healing of crack damage", Proceedings of the 4th International Conference on Self-Healing Materials, Ghent, Belgium, pp. 16-20 June (2013).
11. W. Jeitschko, H. Nowotny and F. Benesovsky, Monatsh. Chem. 95, 178 (1964).
12. B. Liu, J. Y. Wang, J. Zhang, J. M. Wang, F. Z. Li and Y. C. Zhou, Appl, Phys. Lett. 94, 181906 (2009).
13. Y. Bai, X. He, M. Li, Y. Sun, C. Zhu and Y. Li, Solid State Sci. 12, 144 (2010).
14. L. Yang, K. Huang, T. Pu, B. Wang, and M. Luo, "Study the dielectric and optic properties of Ti2XC (X=In, Sn,Al, Cd and Pb) by density function theory", Proceedings of the International Conference on Microwave and Millimeter Wave Technology, pp. 8-11 May (2010).

15. M. F. Cover, O. Warschkow, M. M. M. Bilek and D. R. McKenzie, J. Phys.: Condens. Matter 21, 305403 (2009).
16. S. J. Clark, M. D. Segall, C. J. Pickard, P. J. Hasnip, M. I. J. Probert, K. Refson and M. C. Payne, Zeitschrift für Kristallographie. 220, 567 (2005).
17. P. Hohenberg and W. Kohn, Phys. Rev. 136, B864 (1964).
18. W. Kohn and L. J. Sham, Phys. Rev. 140, A1133 (1965).
19. J. P. Perdew, K. Burke and M. Ernzerhof, Phys. Rev. Lett. 77, 3865 (1996).
20. D. Vanderbilt, Phys. Rev. B 41, 7892 (1990).
21. T. H. Fischer and J. Almlof, J. Phys. Chem. 96, 9768 (1992).
22. H. J. Monkhorst and J. D. Pack, Phys. Rev. B 13, 5188 (1976).
23. F. D. Murnaghan, Finite Deformation of an Elastic Solid (Wiley, New York, 1951).
24. R. Saniz, L. H. Ye, T. Shishidou and A. J. Freeman, Physical Review B 74, 014209 (2006).
25. S. Li, R. Ahuja, M. W. Barsoum, P. Jena and B. Johansson, Appl. Phys. Lett. 92, 221907 (2008).
26. Y. L. Du, Z. M. Sun, H. Hashimoto and M. W. Barsoum, Phys. Lett. A 374, 78 (2009).
27. M. Born, Math. Proc. Camb. Philos. Soc. 36, 160 (1940).
28. S. F. Pugh, Philos. Mag. 45, 823 (1954).
29. J. Haines, J. M. Léger and G. Bocquillon, Annu. Rev. Mater. Res. 31, 1 (2001).
30. W. Y. Ching, Y. Mo, S. Aryal and P. Rulis, J. Am. Ceram. Soc. 96, 2292 (2013).
31. M. A. Hadi, M. Roknuzzaman, F. Parvin, S. H. Naqib, A. K. M. A. Islam and M. Aftabuzzaman, J. Sci. Res. 6, 11 (2014).
32. M. T. Nasir, M. A. Hadi, S. H. Naqib, F. Parvin, A. K. M. A. Islam, M. Roknuzzaman and M. S. Ali, Int. J. Mod. Phys. B 29, 1550022 (2015).
33. G. Hug and E. Fries, Phys. Rev. B 65, 113104 (2002).
34. H. Faraoun, R. Terki, C. Esling and H. Aourag, Mater. Sci. Eng. B 110, 280 (2004).
35. Y. Zhou and Z. Sun, Phys. Rev. 61, 12570 (2000).
36. M. Roknuzzaman and A. K. M. A. Islam, ISRN Condensed Matter Physics 2013, article ID 646042 (2013).
37. Y. L. Du, Z. M. Sun, H. Hashimoto and M. W. Barsoum, Phys. Lett. A 374, 78 (2009).
38. N. Benayad, D. Rached, R. Khenata, F. Litimein, A. H. Reshak, M. Rabah and H. Baltache, Mod. Phys. Lett. B 25, 747 (2011).
39. M. A. Hadi, M. S. Ali, S. H. Naqib and A. K. M. A. Islam, Int. J. Comp. Mater. Sci. Engin. 2, 1350007 (2013).